dielectric constant of the surface layer is comparable with that proposed to explain the switching properties in thin crystals of other ferroelectrics.

By suggesting a possible origin for the surface layer in $KH_2PO_4$-type crystals, we do not mean to imply that other sources of a surface layer, different from the bulk crystal, are not more common. An obvious source of such a layer would be mechanical damage during cutting and polishing operations. Such a layer would probably be of much greater thickness.

While our considerations have been directed toward crystals with vapor-deposited electrodes, precisely the same considerations will account for domain formation when ferroelectrics are immersed in conducting solution. Mitsui and Furuichi found that, for well-annealed Rochelle salt crystals, 180° domain widths are not affected by immersion in a conducting solution until the crystal thickness is less than $\simeq$0.4 mm.[2] Below that thickness the domain widths of crystals immersed in solution are much greater than for unshorted crystals. This may be understood on the basis of our model if, for Rochelle salt crystals less than $\simeq$0.4 mm in thickness, the surface-layer thickness $s$ becomes an appreciable fraction of the total crystal thickness.

PHYSICAL REVIEW VOLUME 159, NUMBER 2 10 JULY 1967

# Kinematic Effects in Spin-$\frac{1}{2}$ Antiferromagnetism*

RICHARD P. KENAN
*Battelle Memorial Institute, Columbus Laboratories, Columbus, Ohio*

(Received 23 January 1967)

A coupled-fermion representation of spin operators is used to examine the effect of the kinematic interaction on the zero-point motion of a spin-$\frac{1}{2}$ antiferromagnet. The calculation is carried through fourth order so that exchange corrections are included. It is shown that the kinematic interaction is not small, but that the combined kinematic-dynamic corrections to the spin-wave theory are small, numerical calculations showing a correction of less than 1% of the spin-wave values.

## I. INTRODUCTION

THE term "kinematic interaction" was introduced by Dyson[1] in his study of spin-wave interactions to characterize certain terms in his boson Hamiltonian. These terms originate in the expansion of spin operators in terms of bosons. The spin-deviation operator $S-S^z$ can have only $2S+1$ values, whereas the boson equivalent operator $a^\dagger a$ is unrestricted. As a result, there appear terms in the expanded Hamiltonian to effect the spin-deviation restriction, in addition to the terms expressing the "dynamic interaction," the direct interaction between spins. An important part of Dyson's spin-wave results is his demonstration that the kinematic terms can be neglected in ferromagnetic systems at low temperatures.

An antiferromagnetic system has the same eigenstates as the corresponding ferromagnetic system, but the energy levels are inverted. The ground state of the antiferromagnet is therefore identical to the highest excited state of the ferromagnet (for zero field), and, as might be expected, is very complicated in its details. Little is known, in fact, about the details of the antiferromagnetic ground state. It is known that the perfectly ordered Neel states ($z$ components of spin alternating in alignment) are not even eigenstates. The ordinary spin-wave theory must therefore be regarded as an approximation even at $T=0$, in contrast to the ferromagnetic case. This situation makes the application of Dyson's technique to antiferromagnetism an almost hopeless task, and the analog of Dyson's work has never been carried out for the antiferromagnetic case. There is, of course, no reason to expect that the kinematic effects should vanish at $T=0$ for antiferromagnetic systems, but the success of the spin-wave theory at low temperatures suggests that these effects should be small.

In the present paper we analyze, by perturbation theory, the low-temperature behavior of the long-range order of an antiferromagnetic system of spins $\frac{1}{2}$. Thermodynamic perturbation theory is used but, because of the flatness of the low-temperature magnetization, it suffices to study only the zero-temperature limit, i.e., the zero-point motion. It is our aim to obtain an estimate of the importance of kinematic effects on this motion. The spin statistics are accounted for by the use of a coupled-fermion representation discussed by Mattis.[2]

The separation of the kinematic parts of the interaction from the dynamic ones is not explicit in the fermion Hamiltonian, so we insert here a few comments on the subject. When the spin Hamiltonian is expanded in the coupled-boson representation used by Dyson, there result terms bilinear in the boson operators, a diagonal term bilinear in the number operators, and several higher-order terms. The bilinear terms taken alone can be diagonalized by use of a simple canonical transformation, resulting in the ordinary linear spin-

* Study supported by the U. S. Air Force Office of Scientific Research Grant No. AF-AFOSR-868-65.

[1] F. J. Dyson, Phys. Rev. **102**, 1217 (1956); **102**, 1230 (1956).

[2] D. C. Mattis, *The Theory of Magnetism* (Harper and Row, Publishers, New York, 1965), pp. 77, 78.

wave theory. The diagonal-interaction term then expresses the direct interaction between two antiferromagnetic spin waves (the dynamic interaction), while the higher-order terms contrive to ensure the operation of the Pauli principle (the kinematic interaction). When the coupled-fermion representation is used, a special set of Fermi operators (which we call "drone operators") is introduced to account for the commutation relations of spin operators attached to distinct lattice sites, while a different set of Fermi operators (which we call "particle operators") accounts for the commutation relations between operators belonging to the same lattice site. Thus, the kinematic interaction is itself split into two parts. The expansion of the Hamiltonian results in terms which are linear and bilinear in the number operators of the particles, and in terms bilinear in both the particle and the drone operators (and therefore quartic over-all). The term bilinear in the number operators for particles expresses all of the dynamic interaction, just as in the boson representation, but it also contains some of the kinematic interaction. The remainder of the terms contain the analog of the spin-wave terms and the rest of the kinematic interaction. We will consider the difference between the zero-point motion predicted by the ordinary spin-wave theory and that predicted by the present theory when the dynamic interaction term is neglected to originate in the kinematic interaction. The dynamic interaction term, of course, does give a nonzero contribution at $T=0$, and we will obtain an estimate of this contribution. The inclusion of these terms will, however, make separation of dynamic and kinematic effects impossible; one can then only make a separation into kinematic and mixed dynamic-kinematic effects.

In outline, the paper is organized as follows. In Secs. II and III, the Hamiltonian is put into the coupled-fermion representation and a fairly standard fermion perturbation expansion is derived. In Sec. IV, the expansion is applied to the long-range order and the graphs are reduced, resulting in an integral equation for the single-particle propagator. In Sec. V, a resummation of kernel graphs over a special class of graphs is performed, and the resulting equations are solved approximately. This procedure gives the ordinary spin-wave theory in lowest order. In Sec. VI, the graphs representing the corrections to the resummed kernel are evaluated through fourth order. Finally, in Sec. VII, the results of numerical calculation of the zero-point motion are presented and discussed. Certain mathematical aspects of the problem are given in the Appendix.

## II. THE HAMILTONIAN

We consider a system of $2N$ spins of magnitude $\frac{1}{2}$ situated in a simple lattice and interacting via Heisenberg exchange between nearest-neighboring atoms. Only lattices which can be decomposed into two interpenetrating sublattices such that the nearest neighbors of an atom in one sublattice all lie in the other are considered. The Hamiltonian is

$$H=2J\sum_{\langle jk\rangle}\mathbf{R}_j\cdot\mathbf{S}_k-\xi\sum_j R_j{}^z+\xi\sum_k S_k{}^z, \tag{1}$$

where $J$ is the exchange integral, $J>0$ for antiferromagnetism, and where $\langle jk\rangle$ indicates that sites $j$ and $k$ are nearest neighbors. The parameter $\xi$ is proportional to a "staggered" internal field, pointing in the $+z$ direction for atoms in the $R$ sublattice and in the $-z$ direction for atoms in the $S$ sublattice. The operators $\mathbf{R}$ and $\mathbf{S}$ satisfy the commutation rules

$$[S_i{}^+,\ S_j{}^-]_-=2\delta_{ij}S_i{}^z; \qquad [S_i{}^z,\ S_j{}^\pm]_-=\pm\delta_{ij}S_i{}^\pm, \tag{2}$$

and, for spin $\frac{1}{2}$,

$$[S_i{}^+,\ S_i{}^-]_+=1, \tag{3}$$

where

$$S^\pm=S^x\pm iS^y. \tag{4}$$

Equation (3) reflects the general property of spin operators,

$$(S^\pm)^{2S+1}=0, \tag{5}$$

and suggests that a fermion representation of the spin operators may be convenient. The only distinction between the operators (4) and fermions is that the spin operators commute for distinct lattice indices. This feature can be incorporated into a coupled-fermion representation of the spin operators by using a device discussed by Mattis.[2] We introduce two sets of Fermi operators, with one operator of each set attached to each lattice site, by the correspondence

$$S_i{}^+\sim a_i{}^\dagger d_i \qquad S_i{}^-\sim d_i a_i \qquad S_i{}^z\sim a_i{}^\dagger a_i-\tfrac{1}{2}, \tag{6a}$$

$$R_i{}^+\sim d_i a_i \qquad R_i{}^-\sim a_i{}^\dagger d_i \qquad R_i{}^z\sim\tfrac{1}{2}-a_i{}^\dagger a_i. \tag{6b}$$

It is easily verified that these correspondences preserve the commutation rules (2) and (3) if

$$d_i=b_i{}^\dagger+b_i; \qquad d_i{}^2=1; \qquad [d_i,\ d_j]_+=2\delta_{ij} \tag{7}$$

$$[a_i,\ a_j{}^\dagger]_+=[b_i,\ b_j{}^\dagger]_+=\delta_{ij}; \qquad [a_i,\ b_j]_+=[a_i,\ b_j{}^\dagger]_+=0. \tag{8}$$

When Eqs. (6) are inserted into the Hamiltonian, we get

$$H=H_0+H_1+H_2, \tag{9}$$

$$H_0=E_0+\epsilon\sum_j a_j{}^\dagger a_j+\epsilon\sum_k a_k{}^\dagger a_k, \tag{10}$$

$$E_0=-\tfrac{1}{2}NJz-N\xi; \qquad \epsilon=Jz+\xi, \tag{11}$$

$$H_1=-J\sum_{\langle jk\rangle}(a_j{}^\dagger a_k{}^\dagger+a_j a_k)\,d_j d_k, \tag{12}$$

$$H_2=-2J\sum_{\langle jk\rangle}a_j{}^\dagger a_j a_k{}^\dagger a_k. \tag{13}$$

## III. PERTURBATION EXPANSION

Having expressed the Hamiltonian in terms of fermions, we can now proceed to develop a perturbation

expansion for the thermodynamic average of an arbitrary product of such operators. The development of the expansion is standard, so we give only an outline. We start by defining

$$\langle\Omega\rangle = Z_0^{-1}\,\mathrm{Tr}(e^{-\beta H_0}\Omega), \qquad Z_0 = \mathrm{Tr}(e^{-\beta H_0})$$
$$\langle\langle\Omega\rangle\rangle = Z^{-1}\,\mathrm{Tr}(e^{-\beta H}\Omega), \qquad Z = \mathrm{Tr}(e^{-\beta H}), \quad (14)$$

where $\beta = 1/kT$ and $\Omega$ is any operator. Further, we define

$$\mathbf{\Omega}(u) = e^{uH}\Omega e^{-uH},$$
$$\Omega(u) = e^{uH_0}\Omega e^{-uH_0}. \quad (15)$$

Then, one has the relations

$$\Omega(u) = U(u)\,\mathbf{\Omega}(u)\,U^{-1}(u),$$
$$\langle\langle\Omega\rangle\rangle = (Z_0/Z)\,\langle U(\beta)\Omega\rangle, \quad (16)$$

where

$$U(u) = e^{uH_0}e^{-uH}. \quad (17)$$

These equations can then be used to derive

$$\langle\langle T[\alpha_1(u_1)\,\alpha_2(u_2)\cdots\alpha_n(u_n)]\rangle\rangle$$
$$= \frac{Z_0}{Z}\sum_{p=0}\frac{(-1)^p}{p!}\int_0^\beta dx_1\cdots\int_0^\beta dx_p$$
$$\times\langle T[H_I(x_1)\cdots H_I(x_p)\alpha_1(u_1)\cdots\alpha_n(u_n)]\rangle, \quad (18)$$

where $H_I = H - H_0$, $T$ is Wick's ordering operator, which arranges the operators in its argument in order of increasing argument from right to left and attaches the signature of the permutation corresponding to the rearrangement, and $\alpha_i$ stands for one of $(a_i, a_i^\dagger, d_i)$. The average on the right-hand side of Eq. (18) consists of a sum of averages of products of creation and annihilation operators, each product containing the $n$ "external" operators $\alpha_i$, and a number $4p$ of operators arising from the interaction terms $H_I$. Each such averaged product can be written as a sum of products of averaged pairs by the use of the thermodynamic analog of Wick's theorem. There are several derivations of such expansions, the simplest being that given by Gaudin.[3] After the use of the "Wick's" theorem, one can derive a system of graphs representing the terms of the expansion and perform a simple but necessary rearrangement of the series to eliminate certain unphysical terms. This last step is called the linked-cluster expansion, and is discussed in detail in standard references.[4] The over-all result is that only connected graphs, i.e., graphs which can be traced in their entirety without lifting one's pencil, are to be counted, and the factor of $Z_0/Z$ in Eq. (18) is canceled off.

For convenience in describing the graphs to be used in the analysis, we introduce the following terminology. An average (in the ensemble of $H_0$) of a pair of operators will be called the "contraction" of the operators; the operators "$a$" will be called "particle" operators, and the operators "$d$" will be called "drone" operators; the interaction $H_1$ will be called the "spin-flip" interaction, while the interaction $H_2$ will be called the "longitudinal" or the "diagonal" interaction. In the graphs, the interactions are represented by wavy lines, the contraction of two particles lines by a directed solid line, the contraction of two drone lines by a directed dashed line, and the external operators $\alpha_i$ by dots. It will be assumed that the external operator product appears under the $T$ sign in Eq. (18) in the order indicated in the Hamiltonian (normal order), i.e., $R$-sublattice operators to the left of $S$-sublattice operators, then particle operators to the left of drone operators, then creation operators to the left of annihilation operators.

A graph consists of $n$ external lines connected to the dots and to the wavy lines and some number of internal lines connected only to the wavy lines. The dots are labeled with the variables $u_i$, the wavy lines with variables $x_i$, and the directed lines with the appropriate lattice indices, lines connected to the two ends of a wavy line being constrained to carry nearest-neighboring indices. The allowed types of interaction vertices are indicated in Fig. 1, in which it should be noted that the particle lines and the drone lines going with a spin-flip interaction are independently required to be either both incoming or both outgoing, with respect to the wavy line. Each dot of a graph is connected to exactly one other dot through an open polygon whose sides are formed by spin-flip-interaction lines and contraction lines of the same type (particle or drone, not mixed) as the external lines connected to the dots. In addition, there may be some number of closed polygons involving only internal lines but otherwise formed in exactly the same way as the open polygons. Finally, there can occur longitudinal interaction lines in which one end is connected to itself through a single contraction line, closed on itself. All contraction lines belong to exactly one polygon, open or closed.

The contribution of a graph is calculated as follows:

(1) For each particle contraction going from $v_i$ to $v_j$, a factor $G_0(v_i - v_j)$ and for each drone contraction

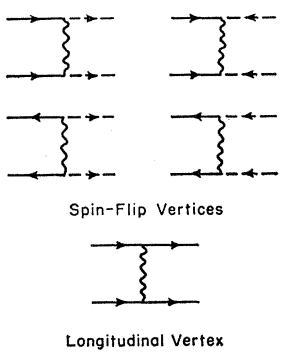


FIG. 1. Allowed interaction vertices.

[3] M. Gaudin, Nucl. Phys. **15**, 89 (1960).
[4] J. Goldstone, Proc. Roy. Soc. (London) **A239**, 267 (1957); J. Hubbard, *ibid.* **A240**, 539 (1957); C. Bloch, Nucl. Phys. **1**, 451 (1958).

from $v_i$ to $v_j$, a factor $\eta(v_i-v_j)$, where $v$ represents $u$ or $x$;

(2) for each spin–flip-interaction line, a factor $+J$, and for each longitudinal interaction line, a factor $+2J$;

(3) for each interaction line of any type, a factor $\delta(\mathbf{k}-\mathbf{j}-\boldsymbol{\delta})$, where $\delta(-)$ is the Kroneker delta, and $\boldsymbol{\delta}$ is one of the set of lattice vectors connecting nearest neighbors, and where $k$ and $j$ are the indices associated with the two ends of the interaction line;

(4) a factor $(-1)^{l+m}$, where $l$ is the number of closed polygons in the graph, and $m$ is defined below;

(5) the product of all these factors is now integrated over the internal variables, $x_i$, from 0 to $\beta$, and a summation over the nearest-neighboring pairs of lattice indices associated with the interaction lines is carried out.

Here,

$$\begin{aligned} G_0(v_i-v_j) &\equiv \langle T[a_i^\dagger(v_i)a_j(v_j)]\rangle \\ &= \exp[\epsilon(v_i-v_j)]\langle a_i^\dagger a_i\rangle\delta_{ij} \qquad \text{if } v_i>v_j \\ &= -\exp[\epsilon(v_i-v_j)]\langle a_i a_i^\dagger\rangle\delta_{ij} \qquad \text{if } v_i<v_j, \end{aligned} \tag{19}$$

$$\begin{aligned} \eta(v_i-v_j) &= +1 \qquad \text{if } v_i>v_j \\ &= -1 \qquad \text{if } v_i<v_j, \end{aligned} \tag{20}$$

and the factor $m$ is determined as follows: If there are no drone open polygons containing an odd number of drone lines, then $m=0$. If there are one or more such polygons, each must be examined individually. Each of these polygons has one incoming and one outgoing external line. If the operator corresponding to the incoming line lies to the left of the operator corresponding to the outgoing line in the original product $\pi\alpha_i(u_i)$, then the $m$ value for that polygon is zero, otherwise it is unity. This examination is necessitated by an ambiguity in the definition of normal order caused by the fact that the drone operators are Hermitian.

## IV. LONG-RANGE ORDER

For spin-$\frac{1}{2}$ systems, the long-range order may be defined as

$$\sigma=\langle\langle 1-2a^\dagger a\rangle\rangle=2\langle\langle\,|\,s^z\,|\,\rangle\rangle, \tag{21}$$

where the lattice index has been omitted because the translational invariance of the lattice makes averages of operators subscripted with only one lattice index independent of the index. We are therefore interested in the average $\langle\langle a^\dagger a\rangle\rangle$, which may be found by application of the perturbation theory discussed in Sec. III to the single-particle propagator

$$G(u_1-u_2)=\langle\langle T[a_i^\dagger(u_1)a_i(u_2)]\rangle\rangle. \tag{22}$$

This is, in fact, the only nonvanishing average of two-particle operators because of the way in which the drone operators enter the interaction Hamiltonian.

The graphs contributing to $G$ all have one incoming and one outgoing particle-contraction line. The drone operators, if they appear at all, are contracted in closed polygons. In general, there will occur places within these graphs where the removal of a single particle-contraction line will cause the graph to fall into two disconnected pieces; we say that the graph is reducible at this line. Because of the way in which the drone operators enter the interaction terms, the lines at which a graph is reducible all carry the same lattice index as the external lines. A typical graph contributing to $G$ consists of several contraction lines at which the graph is reducible, connected by graph parts containing no such lines, i.e., graph parts which cannot be reduced. We call the irreducible parts "kernel pieces" and denote the sum of all kernel pieces by $K'(x_1-x_2)$. Let us lay out the graphs contributing to $G$ horizontally, with the incoming external line on the left and the outgoing external line on the right, and focus our attention on the leftmost kernel piece. To the right of this kernel piece is another graph contributing to $G$. Hence, summing over kernel pieces in the leftmost position, and over graphs contributing to $G$ on its right, we arrive at the integral equation

$$\begin{aligned} G(u_1-u_2) &= G_0(u_1-u_2)+\int_0^\beta dx_1\int_0^\beta dx_2 \\ &\quad\times G_0(u_1-x_1)K(x_1-x_2)G(x_2-u_2) \\ &\quad+\int_0^\beta G_0(u_1-x_1)K_0G(x_1-u_2)\,dx_1, \end{aligned} \tag{23}$$

where $K_0$ is the constant part of $K'$, i.e., that part of $K'$ which is attached to the external-line open polygon by exactly one (longitudinal) interaction line, and $K=K'-K_0$. This integral equation represents an elementary resummation of the perturbation series which takes into account multiple returns of the spin deviation to the same lattice site.

The cyclic invariance of the trace operation by which the average in $G$ is defined requires that $G_0$, $G$, and $K$ be antiperiodic functions of their arguments in the interval $[-\beta,\beta]$, with period $\beta$, i.e., if $F(r)$ represents one of them, then we have

$$F(r-\beta)=-F(r), \qquad 0\le r\le\beta. \tag{24}$$

Since the functions are defined only in the interval $[-\beta,\beta]$, we can extend them periodically outside this interval and expand the resulting functions in a Fourier series:

$$F(r)=\sum_{-\infty}^{\infty}{}_m f(m)\,\exp(i\pi mr/\beta), \quad m \text{ odd}, \tag{25}$$

$$f(m)=(2\beta)^{-1}\int_{-\beta}^{\beta}F(r)\,\exp(-i\pi mr/\beta)\,dr. \tag{26}$$

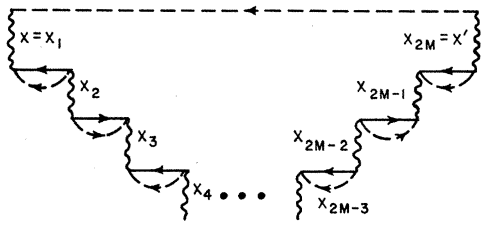


FIG. 2. Form of the graphs included in $K_s$.

The integral equation (26) then becomes

$$g(m)=g_0(m)+\beta^2 g_0(m)k(m)g(m)+\beta K_0 g_0(m)g(m), \tag{27}$$

an algebraic equation. The Fourier coefficient $g_0(m)$ is given by

$$g_0(m)=-(\epsilon\beta-im\pi)^{-1}, \quad m \text{ odd}. \tag{28}$$

## V. PARTIAL RESUMMATION OF PERTURBATION SERIES

In this section, we perform a summation over a special class of kernel parts. These parts all have the form illustrated in Fig. 2, with all internal particle contraction lines bracketed by a drone line. This bracketing of the internal particle lines has the effect of eliminating the normally strong statistical interference between two particle lines which may belong to the same lattice site. This lack of interference is characteristic of bosons, which leads us to suspect that these graphs may contain the spin-wave contribution.

The contribution to $K$ from the graph of Fig. 2, containing $2M$ spin-flip interactions, is given by

$$\begin{aligned}K_{2M}(x-x')=&-(Jz)^{2M}S(2M)\\ &\times\int_0^\beta dx_2\cdots\int_0^\beta dx_{2M-1}G_0(x_2-x)\eta(x_2-x)\\ &\times G_0(x_2-x_3)\eta(x_2-x_3)\cdots G_0(x'-x_{2M-1})\\ &\times\eta(x'-x_{2M-1})\eta(x'-x),\end{aligned} \tag{29}$$

where $S(2M)$ is given by

$$S(2M)=N^{-1}\sum_{\mathbf{k}}\gamma_{\mathbf{k}}^{2M}; \qquad \gamma_{\mathbf{k}}=z^{-1}\sum_{\boldsymbol{\delta}}\exp(i\mathbf{k}\cdot\boldsymbol{\delta}), \tag{30}$$

as is shown in the Appendix. Introducing the Fourier expansion for the product $\eta(r)G_0(r)m$,

$$\mathfrak{F}\{\eta(r)G_0(r)\}=\sigma_0(\epsilon\beta-il\pi)^{-1}, \quad l \text{ even}, \tag{31}$$

into Eq. (32) gives

$$\begin{aligned}K_{2M}(x-x')=&-(Jz)^{2M}S(2M)\beta^{2M-2}\sum_{m_1m_2(\text{odd})}\exp[i\pi m_1(x-x')/\beta]\\ &\times\left|\frac{\sigma_0}{\epsilon\beta-i(m_1+m_2)\pi}\right|^{2M-2}\frac{\sigma_0}{\epsilon\beta+i(m_1+m)\pi}\eta(m_2),\end{aligned} \tag{32}$$

where

$$\eta(m)=2/im\pi, \quad m \text{ odd}. \tag{33}$$

Using Eq. (33), then, we find

$$\begin{aligned}k_{2M}(m)=&-N^{-1}\sum_{\mathbf{k}}\sum_{m'}\left|\frac{\sigma_0\beta Jz\gamma_{\mathbf{k}}}{\epsilon\beta-i(m+m')\pi}\right|^{2M-2}\\ &\times\frac{\sigma_0(Jz\gamma_{\mathbf{k}})^2}{\epsilon\beta+i(m+m')\pi}\eta(m').\end{aligned} \tag{34}$$

Summing this from $M=1$ to $M=\infty$ gives the contribution of all kernel pieces in the class, which we denote by $k_s$:

$$k_s=-\frac{\sigma_0}{N}\sum_{\mathbf{k}}\sum_{m'}(Jz\gamma_{\mathbf{k}})^2\frac{[\epsilon\beta-i(m+m')\pi]\eta(m')}{(\beta\varphi)^2+(m+m')^2\pi^2}, \tag{35}$$

where

$$\varphi^2=\epsilon^2-(\sigma_0 Jz\gamma_{\mathbf{k}})^2 \tag{36}$$

is the usual spin-wave dispersion curve near $T=0$, where $\sigma_0=1$.

The summation over $m'$ in Eq. (35) can be carried out by elementary methods,[5] giving

$$\begin{aligned}&k_s(m)\\ &=-\frac{i\sigma_0}{2N}\sum_{\mathbf{k}}(Jz\gamma_{\mathbf{k}})^2\frac{\coth\frac{1}{2}\beta\varphi}{\varphi}\left[\frac{\epsilon+\varphi}{m\pi-i\beta\varphi}+\frac{\epsilon-\varphi}{m\pi+i\beta\varphi}\right].\end{aligned} \tag{37}$$

When Eq. (40) is inserted into Eq. (27), there results

$$\begin{aligned}g_s(\omega_m)=\beta^{-1}\Bigg(&\omega_m-\epsilon-\frac{\sigma_0}{2N}\sum_{\mathbf{k}}(Jz\gamma_{\mathbf{k}})\frac{2\coth\frac{1}{2}\beta\varphi}{\varphi}\\ &\times\left[\frac{\epsilon+\varphi}{i\omega_m+\varphi}+\frac{\epsilon-\varphi}{i\omega_m-\varphi}\right]\Bigg)^{-1},\end{aligned} \tag{38}$$

where

$$\omega_m=m\pi/\beta. \tag{39}$$

The usual procedure now would be to continue $\omega_m$ into the complex plane and use standard methods[6] to derive from Eq. (38) a spectral function, from which the thermodynamics of the system described by $g_s$ can be determined. In practice, this procedure is virtually impossible to carry out, because the way in which the summations over $k$ enter into $g_s$ makes the determination of the poles of $g_s$ equivalent to the solution of an algebraic equation of degree $2N+1$. Instead, we will simply accept the iterated solution

$$g_s(m)=g_0(m)+\beta^2 g_0k_sg_0(m)+\beta^4(g_0k_s)^2g_0(m)+\cdots. \tag{40}$$

The evaluation of the contribution of the $l$th iteration in (40) to the average spin deviation per site is straight-

[5] The procedure is reviewed in the appendix of K. Tomita, Proc. Phys. Soc. (London) **88**, 293 (1966).

[6] D. N. Zubarev, Usp. Fiz. Nauk **71**, 71 (1960) [English transl. Soviet Phys.—Usp. **3**, 320 (1960)].

forward but tedious. Denoting this contribution by $n_l$, we find after much algebra

$$n_l=\frac{1}{2}\left(\frac{\sigma_0}{2N}\right)^l\sum_{\mathbf{k}_1}f(\mathbf{k}_1)\cdots\sum_{\mathbf{k}_l}f(\mathbf{k}_l)\,\mathcal{S}\sum_{j=1}^{l}C_j(\varphi_1\cdots\varphi_l)$$
$$\times\left[\frac{\tanh\frac{1}{2}\beta\varphi_j}{(\epsilon+\varphi_j)^l}+\frac{(-1)^l}{l!}\frac{d^l}{dz^l}\frac{\tanh\frac{1}{2}\beta z}{(z+\varphi_j)}\right],\qquad z=\epsilon \quad (41)$$

where $\varphi_j=\varphi(\mathbf{k}_j)$,

$$C_j(\varphi_1\cdots\varphi_l)=\prod_{i=1,i\neq j}^{l}\frac{\epsilon+\varphi_i}{\varphi_j-\varphi_i},$$

$$f(\mathbf{k})=\frac{(Jz\gamma_{\mathbf{k}})^2\coth\frac{1}{2}\beta\varphi(\mathbf{k})}{\varphi(\mathbf{k})}, \quad (42)$$

and where the symbol $\mathcal{S}$ means that the result is to be symmetrized with respect to the $\varphi_j$. The total spin deviation is then given by

$$n=\langle\langle a^\dagger a\rangle\rangle=\langle a^\dagger a\rangle+\sum_{l=1}n_l. \quad (43)$$

At low temperatures, $n$ is not strongly temperature-dependent, and its value is well approximated by the zero-point deviation, determined by

$$n_l^0=\left(\frac{1}{2N}\right)^l\sum_{\mathbf{k}_1}f(\mathbf{k}_1)\cdots\sum_{\mathbf{k}_l}f(\mathbf{k}_l)\,\mathcal{S}$$
$$\times\sum_{j=1}^{l}C_j(\varphi_1\cdots\varphi_l)\frac{\theta(\varphi_j)}{(\epsilon+\varphi_j)^l}, \quad (44)$$

where $\theta(x)$ is the Heavyside unit step. The presence of the symbol $\mathcal{S}$ makes even this simple expression tedious to evaluate. The term for $l=1$ gives the spin-wave result

$$n_{swt}^0=n_1^0=(2N)^{-1}\sum_{\mathbf{k}}[\epsilon/\varphi(\mathbf{k})-1]. \quad (45)$$

The term for $l=2$ gives the lowest-order kinematic corrections to the spin-wave theory

$$n_2^0=\frac{1}{2N^2}\sum_{\mathbf{k}_1\mathbf{k}_2}\left[\frac{(\epsilon+\varphi_1)(\epsilon-\varphi_1)^2}{\varphi_1}\frac{1}{\varphi_1+\varphi_2}\frac{\epsilon-\varphi_2}{\varphi_2(\epsilon+\varphi_2)}\right]$$
$$-\frac{1}{2}\left[-N^{-1}\sum_{\mathbf{k}}\frac{(\epsilon-\varphi)}{\varphi(\epsilon+\varphi)}\right]\left[N^{-1}\sum_{\mathbf{k}}\frac{(\epsilon^2-\varphi^2)}{\varphi}\right]-(n_1^0)^2. \quad (46)$$

Higher-order terms are increasingly complex and we will not consider them because they are expected to give only a small contribution.

## IV. LOW-ORDER CORRECTIONS TO $K_s$

In this section we will calculate some low-order corrections to $K_s$, taking the calculations through fourth order. We choose fourth order because that is the first order in which graphs containing exchange among the drone lines occur. It is important to obtain an estimate

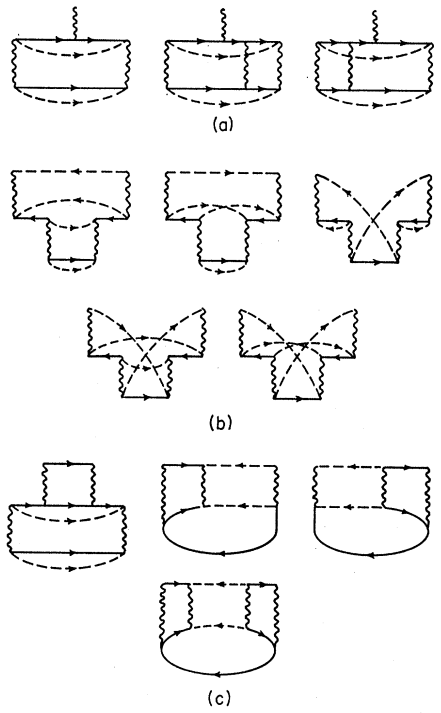


FIG. 3. (a) Graphs included in $K_0$; (b) fourth-order exchange graphs; (c) mixed graphs.

of the contribution of such graphs because they are the graphs which correct $K_s$, and therefore $G_s$, for the commutation relations of the spin operators. $K_s$ itself, of course, already contains strong correction terms of this sort, expressed by the noninterference of the internal-particle lines.

We are interested here in the low-temperature properties (in fact, we are considering only the zero-point motion in the final analysis), so any graph which contains one or more factors of $\langle a^\dagger a\rangle$ can be ignored. This enables us to discard any graph which contains a closed-particle loop which connects only to longitudinal interaction lines, and any graph which contains a pair of oppositely directed particle lines connected to the same pair of interaction vertices. The remaining graphs which contribute near $T=0$ can then be divided into three classes. The graphs which give $K_0$ are illustrated in Fig. 3(a); the drone-exchange graphs are illustrated in Fig. 3(b), and the remaining graphs which contribute near $T=0$ are illustrated in Fig. 3.

The graphs of Fig. 3(a) contribute to $K_0$. When they are introduced into the transformed integral equation, Eq. (27), they produce a shift in the energy $\epsilon$ carried by the propagator $g_0$ in the equation, which can then be rewritten in the form

$$g=\bar{g}_0+\beta^2\bar{g}_0kg, \quad (47)$$

where

$$\bar{g}_0=-[(\epsilon+K_0)\beta-im\pi]^{-1}. \quad (48)$$

It should be noted that it is possible to eliminate $K_0$

TABLE I. Corrections to the spin-wave value of the zero-point motion. In the first column is given the nomenclature used for the terms shown in the second column. The subscripts refer to the kernel part from which the terms arise, while the superscripts refer to the order, in the iterated solution, in which the term occurs. Thus, $n_s^{(2)}$ is the contribution from $k_s$ alone in the second iterate. The third column gives the expressions resulting from the Fourier inversion. The functions $S_0$ and $F_l(\mu)$ are defined in the text.

| | | |
|---|---|---|
| $n_s^{(1)}$ | $\beta^2 g_0^2 k_s$ | $(2N)^{-1}\sum_{\mathbf{k}} (1-\varphi)/\varphi$ |
| $n_m^{(1)}$ | $\beta^2 g_0^2 k_m$ | $(2+1/z)/(4z^2)$ |
| $n_{ex}^{(1)}$ | $\beta^2 g_0^2 k_{ex}$ | $-3(1+1/z)/(16z^2)$ |
| $n_s^{(2)}$ | $\beta^4 g_0^3 k_s^2$ | $S_0-1/2\,S_1S_2-(n_s^{(1)})^2$ |
| $n_{ms}^{(2)}$ | $2\beta^4 g_0^3 k_m k_s$ | $8[F_0(3)-(2+1/z)F_0(-1)]$ |
| $n_{ex\,s}^{(2)}$ | $2\beta^4 g_0^3 k_{ex} k_x$ | $2[4F_0(-3)/z-F_0(1)$ $-2\epsilon\beta(1+2/z)F_1(-1)$ $+(1-2/z)F_0(-1)]$ |
| $n_{ks}^{(2)}$ | $2\beta^3 k_0 g_0^3 k_s$ | $(1+1/z)\,S_2/(2z)$ |
| $n_{km\,ex}^{(2)}$ | $2\beta^3 k_0 g_0^3 (k_m+k_{ex})$ | $(1+1/z)\,(1-1/8z)/(2z)^3$ |

from consideration entirely by introducing an internal field as suggested by Mills *et al.*,[7] and as was done by Kenan.[8] However, one then finds that the function $\varphi$ occuring in $K_s$ can become imaginary for some values of $\mathbf{k}$, corresponding to long wavelengths. Furthermore, the boundary between real and imaginary values of $\varphi$ is some surface in the Brillouin zone, making both physical interpretation and numerical work rather difficult. Similar difficulties arise in the use of Eqs. (47) and (48), because $k_0$ is negative. For our purposes, it is sufficient to account for $K_0$ explicitly as it appears in Eqs. (23) and (27).

The graphs of Fig. 3(a) give for $K_0$:

$$K_0=-\tfrac{1}{4}J(Jz/\epsilon)^2[1+\sigma_0(J/\epsilon)][2\sigma_0-\epsilon\beta(1-\sigma_0^2)]. \quad (49)$$

The exchange graphs shown in Fig. 3(b) are most easily evaluated by direct integration, as are also the mixed graph[5] of Fig. 3(c). The algebra involved is somewhat tedious and entirely unilluminating; we will not include it, but instead we quote the answer. Denoting the contribution of the exchange graphs by $K_{ex}$ and that of the mixed graph[5] by $K_m$, we find

$$K_{ex}=(4A/z)G_0^3(-r)+C(r)G_0(-r)-\sigma_0^2AG_0(r), \quad (50)$$

and

$$K_m=4AG_0^3(r) -A(1-\sigma_0^2)[1+2\epsilon[r-\tfrac{1}{2}\beta\eta(r)]+\tfrac{1}{2}(\sigma_0\beta)]G_0(r) -4A(2+1/z)G_0(-r), \quad (51)$$

where

$$A=(Jz)^4/4\epsilon^2z^2, \quad (52)$$

and

$$C(r)=A\{[\sigma_0\epsilon\beta(1+2/z)+\sigma_0^2(1-1/z)-1/z] +2\epsilon[\sigma_0^2(1+1/z)+1/z][r-\tfrac{1}{2}\beta\eta(r)]\}. \quad (53)$$

The Fourier coefficients of these functions are easily evaluated in terms of

$$g_{03}(m)=-(3\epsilon\beta-im\pi)^{-1}. \quad (54)$$

We find near $T=0$ and for zero field:

$$k_{ex}=(4A/z)\,g_{03}^*(m)-Ag_0(m) -2\epsilon\beta A(1+2/z)[g_0^*(m)]^2+A(1-2/z)\,g_0^*(m) \quad (55)$$

and

$$k_m=4A[g_{03}(m)-(2+1/z)\,g_0^*(m)]. \quad (56)$$

In Sec. VII, numerical results for the contribution of $K_s$, $K_{ex}$, and $K_m$ to the zero-point deviation will be displayed and discussed.

## VII. NUMERICAL RESULTS AND CONCLUSIONS

The evaluation of $G$ by Fourier inversion of $g$ using the kernel given by $K_0$ and the sum of Eqs. (37), (55), and (56) is a hopeless task because of the complexity of $k_s$. For our purposes it suffices to use the iterated solution of Eq. (40), taken through the second iterate. It is expected that the principal error committed here will be in the neglect of higher-order terms in $k_s$ and $K_0$, since $k_s$ is at least of order $1/z$, and $K_0$ is of order $1/z$, while $k_{ex}$ and $k_m$ are both of order $1/z^2$. The second iterate is chosen as terminating point because the cancellation occurring between kinematic and dynamic effects is clearly demonstrated at this level, while the terms arising from $k_s$ remain tractable. The approximate form of Eq. (40) to be used is, then,

$$g\cong g_0+\beta g_0^2K_0+\beta^2g_0^2k+\beta^2g_0^3K_0+\beta^4g_0^3k^2+2\beta^3K_0g_0^3k. \quad (57)$$

The first, second, and fourth terms here contribute

TABLE II. Numerical values of the various corrections to the spin-wave zero-point motion for the NaCl ($z=6$) and the CsCl ($z=8$) lattices. $n_s^{(1)}$ is the spin-wave value, displayed here for comparison with the corrections.

| Term | NaCl | CsCl |
|---|---|---|
| $n_s^{(1)}$ | 0.0761 | 0.0587 |
| $n_m^{(1)}$ | 0.0150 | 0.0083 |
| $n_{ex}^{(1)}$ | −0.0061 | −0.0033 |
| $n_s^{(2)}$ | −0.0132 | −0.0078 |
| $n_{ms}^{(2)}$ | −0.0074 | −0.0033 |
| $n_{ex\,s}^{(2)}$ | 0.0019 | 0.0009 |
| $n_{ks}^{(2)}$ | 0.0094 | 0.0053 |
| $n_{km\,ex}^{(2)}$ | 0.0007 | 0.0003 |
| Total correction to $n_s^{(1)}$ | +0.0004 | +0.0002 |

[7] R. L. Mills, R. P. Kenan, and J. Korringa, Physica **26**, S-204 (1960).

[8] R. P. Kenan, in *Proceedings of the Eighth International Conference on Low-Temperature Physics, London, 1962*, edited by R. O. Davies (Butterworths Scientific Publications Ltd., London, 1963).

nothing at $T=0$ because

$$\sum_{\text{m odd}} g_0^{l+1}(m)=[(\epsilon\beta)^{-l}/2l!]\tanh^{(l)}\tfrac{1}{2}\epsilon\beta, \tag{58}$$

which vanishes for $\beta\to\infty$. The remaining terms give rise to eight sums which we display in Table I. The terms quadratic in $k_{ex}$ or $k_m$ and the term in $k_{ex}k_m$ have been omitted as being of order smaller than $1/z^4$. The sums $S_0$, $S_1$, $S_2$, and the function $F_l(\mu)$ referred to in the table are

$$S_0=\frac{1}{2N^2}\sum_{k_1}\sum_{k_2}\frac{1-\varphi_1}{\varphi_1(1+\varphi_1)}\frac{1}{\varphi_1+\varphi_2}\frac{(1-\varphi_2)^2(1+\varphi_2)}{\varphi_2}, \tag{59}$$

$$S_1=N^{-1}\sum_{k}(1-\varphi^2)/\varphi, \tag{60}$$

$$S_2=N^{-1}\sum_{k}(1-\varphi)/\varphi(1+\varphi), \tag{61}$$

$$F_l(\mu)=\frac{(-\epsilon\beta)^{-l}}{16z^2}[\eta(\mu)]^{l+1}\mathcal{S}N^{-1}\sum_{k}\frac{\gamma_k^2}{|\varphi|}(1+\varphi)\,T_l(\mathbf{k},\mu), \tag{62}$$

$$\begin{aligned}T_l(\mathbf{k},\mu)=&\frac{\eta(\varphi)}{(1+\varphi)^3(\mu+\varphi)^{l+1}}-(-1)^l\\&\times\left[\frac{1}{(1+\varphi)^3(1-\mu)^{l+1}}+\frac{l+1}{(1+\varphi)^2(1-\mu)^{l+2}}\right.\\&\left.+\frac{(l+1)(l+2)}{2}\frac{1}{(1+\varphi)(1-\mu)^{l+3}}\right]\\&+\eta(\mu)\sum_{r=0}^{l}\binom{r+2}{2}\frac{(-1)^r}{(\mu+\varphi)^{l-r+1}(1-\mu)^{r+3}},\quad \mu\neq 1,\end{aligned} \tag{63}$$

$$T_l(k,1)=(1+|\varphi|)^{-l-3}(1+\varphi)^{-1}. \tag{64}$$

In these formulas, we have taken $\xi=0$ so that $\epsilon=Jz$, and have redefined $\varphi$ as $\varphi/\epsilon$; the symbol $\mathcal{S}$ again means that the factors to its right are to be symmetrized with respect to $\varphi$, i.e.,

$$\mathcal{S}F(\varphi)=F(\varphi)+F(-\varphi). \tag{65}$$

The sums over vectors $\mathbf{k}$ are taken over the first Brillouin zone of the sublattice. The triple integral which results from

$$N^{-1}\sum_{k}F\xrightarrow[N\to\infty]{}\frac{1}{(2\pi)^3}\int_{BZ}d^3\mathbf{k}F(k), \tag{66}$$

can be approximated directly by quadratures using a computer. However, such codings are rather slow in execution; furthermore, the double sum in $S_0$ goes into a sixfold integral, which would lead to a prohibitively slow program. Since the most important feature of the dispersion relation

$$\epsilon_{\mathbf{k}}=\epsilon\varphi_{\mathbf{k}} \tag{67}$$

is the curvature and not the angular dependence on $\mathbf{k}$, we have chosen to approximate the integrals using the function

$$\bar{\gamma}_k=\sin|\delta||k|/|\delta||k|, \tag{68}$$

which results from averaging $\gamma_{\mathbf{k}}$ over the directions of $k$. The sum over $k$ then becomes a single integral over $|k|$, while $S_0$ becomes a double integral. This procedure has been used by Mills *et al*[9] with good accuracy.

The integrals shown in Table I have been approximated numerically using a computer (CDC 3400); the results are displayed in Table II. There are two features of this table which we wish to emphasize. First, the purely kinematic corrections to the spin-wave theory ($n_s^{(1)}$), given by

$$n_{\text{kin}}=n_{\text{ex}}^{(1)}+n_s^{(2)}+n_{\text{exs}}^{(2)} \tag{69}$$

are not small, being about 23% and 18% of $n_s^{(1)}$ for the NaCl and CsCl lattices, respectively. Second, the mixed kinematic-dynamic corrections, given by

$$n_{\text{mixed}}=n_m^{(1)}+n_{ms}^{(2)}+n_{ks}^{(2)}+n_{kmex}^{(2)} \tag{70}$$

almost exactly cancel the kinematic ones, the residual corrections being 0.5% and 0.3% for the two lattices. The result is that the spin-wave theory is a good approximation. Furthermore, the corrections which arise when finite temperatures are considered are all of order $\langle a^\dagger a\rangle\cong e^{-\beta\epsilon}$ for $\beta$ large, so these effects should only begin to be significant when $T$ becomes an appreciable fraction of, say, the molecular-field transition temperature, $T_N$ (where $\epsilon\beta=2$). If we presume that the coefficient of $e^{-\epsilon\beta}$ in the temperature-dependent part of the long-range order is of the same order of magnitude as the zero-point motion, then we find that these corrections are as large as 1% only for $\epsilon\beta\lesssim 5$, which is about 40% of $T_N$. While this analysis can hardly be termed accurate, nonetheless it should soften some of the surprise often expressed over the observed wide range of temperature over which the simple spin-wave theory agrees with experiment.

Finally, it should be remarked that although we have included all terms of consequence near $T=0$, through fourth order, our treatment of the integral equation itself is somewhat less precise. Our aims have been to demonstrate that kinematic effects are not particularly small in the Heisenberg antiferromagnet and to display the cancellation between these effects and dynamic effects at low temperatures. The cancellation may be less exact when the complete integral equation is used or when higher-order terms are included in the kernels. Walker[10] has carried out a perturbative treatment of the ground-state problem and finds some disagreement with the spin-wave theory, but he does not, unfortu-

[9] R. E. Mills, R. P. Kenan, and F. J. Milford, Phys. Rev. **145**, 704 (1966).

[10] L. R. Walker, in *Proceedings of the International Conference on Magnetism* (The Institute of Physics and The Physical Society, London, 1964), p. 21.

nately, give any numbers with which we may compare. In any event, it would be surprising if the cancellation we have shown were to become inoperative to any very severe extent in higher-order calculations.

## APPENDIX: LATTICE SUMS

The contribution of any graph to the perturbation expansion consists in part of a summation over the nearest-neighboring pairs of lattice vectors with which the interactions are labeled. The summation is restricted by the topology of the graph via the Kroneker deltas introduced by the particle and drone contraction lines, and by the requirement that the vectors occur in *nn* pairs, introduced by the interaction lines. In order to accommodate the first restriction, we note that the graphs all consist of loops of contraction lines, either connecting external lines (open loops) or closed on themselves (closed loops). The various loops of a graph are connected to one another via the interaction lines (these loops should not be confused with the open and closed polygons defined earlier, which may have spin-flip-interaction lines as part of their perimeter. The present loops have only contraction lines in their perimeter.) All of the lines in a loop carry the same lattice vector. The second restriction on the sums can be accounted for by introducing the representation of a Kroneker delta as a summation over the reciprocal lattice space

$$\sum_{\boldsymbol{\delta}}\delta(\mathbf{i}-\mathbf{j}-\boldsymbol{\delta})=N^{-1}\sum_{\mathbf{k},\boldsymbol{\delta}}\exp[i\mathbf{k}\cdot(\mathbf{i}-\mathbf{j}-\boldsymbol{\delta})]$$
$$=(z/N)\sum_{\mathbf{k}}\gamma_{\mathbf{k}}\exp[i\mathbf{k}\cdot(\mathbf{i}-\mathbf{j})], \quad \text{(A1)}$$

where $\gamma_{\mathbf{k}}$ is defined in (30). The summation over the lattice vectors of the closed loops will then give Kroneker deltas in the $\mathbf{k}$'s, and the exponential factors arising from the open loops will give phase factors which depend only on the differences of the lattice vectors of the open loops. In terms of a prescription, we have:

(1) label the loops with lattice vectors;

(2) for each interaction line connecting loops $\mathbf{i}$ and $\mathbf{j}$, include a factor

$$z/N\sum_{\mathbf{k}}\gamma_{\mathbf{k}}\exp i\mathbf{k}\cdot(\mathbf{i}-\mathbf{j}) \quad \text{(A2)}$$

in the summand;

(3) perform a summation over the lattice vectors of the closed loops and a simplify the resulting expression.

For the graphs which contribute to the magnetization, we can make the prescription somewhat simpler. These graphs have only one open loop, and are therefore not dependent on the lattice vector of this loop. As a result, one can use the following prescription:

(1) For each interaction line, a factor $\gamma_{\mathbf{k}_i}$, where $i$ enumerates the interaction vertices;

(2) for each closed loop, a Kroneker delta in the sum of all the $\mathbf{k}$ vectors associated with interaction lines that touch the loop;

(3) an over-all factor of $N^{I-+L}$, where $I$ is the number of interaction lines, and $L$ is the number of closed loops in the graph.

Summation over the $\mathbf{k}$ vectors then gives the desired lattice sum. The use of the sum of the $\mathbf{k}$ vectors in step 2 above is justified by the inversion symmetry of the lattices under consideration.

The fact that the lattice sum for the graphs contributing to the magnetization (or long-range order) involve only the functions $\gamma_{\mathbf{k}}$ implies that they can all be expressed as products of simple sums,

$$S(2M)=N^{-1}\sum_{\mathbf{k}}\gamma_{\mathbf{k}}{}^{2M}, \quad \text{(A3)}$$

multiplied by powers of $z$. Further, application of the prescription to the graphs of Fig. 2 shows that the lattice sum for these graphs are simply $z^{2M}S(2M)$. It is intuitively clear that the $S(2M)$ are the largest sums that can occur in order $2M$, since the graphs from which they arise contain the least restrictive closed loops. This can also be proved directly by using the expressions given by Kubo[11] for the sums

$$S_{2M}=\left[2^{-2M}\binom{2M}{M}\right]^3 \text{ CsCl lattice}, \quad \text{(A4)}$$

$$S_{2M}=3^{-2M}2^{-2M}\binom{2M}{M}\sum_{l=0}^{M}\binom{2l}{l}\binom{M}{l}^2 \text{ NaCl lattice}. \quad \text{(A5)}$$

Bounds on the lattice sums can be obtained by noting that

$$S(2M)<S(2M-2) \text{ and } S(2M)>S(2)\cdot S(2M-2)$$

from which, since $S(2)=1/z$,

$$S(2M-2)>S(2M)>S(2M-2)/z. \quad \text{(A6)}$$

---

[11] Ryogo Kubo, Phys. Rev. **87**, 568 (1952).